2013

Presynaptic to postsynaptic relationships of the neuromuscular junction are held constant across age and muscle fiber type

Michael R. Deschenes
William & Mary, mrdesc@wm.edu

Taylor E. Hurst
William & Mary

E. Grace Sherman
William & Mary

Amy E. Ramser
William & Mary

Recommended Citation

Deschenes, M. R., Hurst, T. E., Ramser, A. E., & Sherman, E. G. (2013). Presynaptic to postsynaptic relationships of the neuromuscular junction are held constant across age and muscle fiber type. Developmental neurobiology, 73(10), 744-753.

Presynaptic to Postsynaptic Relationships of the Neuromuscular Junction are Held Constant Across Age and Muscle Fiber Type

Michael R. Deschenes,[1,2] Taylor E. Hurst,[1] Amy E. Ramser,[2] E. Grace Sherman[1]

[1] Department of Kinesiology and Health Sciences, The College of William and Mary, Williamsburg, Virginia 23187-8795

[2] Program in Neuroscience, The College of William and Mary, Williamsburg, Virginia 23187-8795

Received 11 March 2013; revised 10 May 2013; accepted 14 May 2013

ABSTRACT: **The neuromuscular junction (NMJ) displays considerable morphological plasticity as a result of differences in activity level, as well as aging. This is true of both presynaptic and postsynaptic components of the NMJ. Yet, despite these variations in NMJ structure, proper presynaptic to postsynaptic coupling must be maintained in order for effective cell-to-cell communication to occur. Here, we examined the NMJs of muscles with different activity profiles (soleus and EDL), on both slow- and fast-twitch fibers in those muscles, and among young adult and aged animals. We used immunofluorescent techniques to stain nerve terminal branching, presynaptic vesicles, postsynaptic receptors, as well as fast/slow myosin heavy chain. Confocal microscopy was used to capture images of NMJs for later quantitative analysis. Data were subjected to a two-way ANOVA (main effects for myofiber type and age), and in the event of a significant ($p < 0.05$) F ratio, a post hoc analysis was performed to identify pairwise differences. Results showed that the NMJs of different myofiber types routinely displayed differences in presynaptic and postsynaptic morphology (although the effect on NMJ size was reversed in the soleus and the EDL), but presynaptic to postsynaptic relationships were tightly maintained. Moreover, the ratio of presynaptic vesicles relative to nerve terminal branch length also was similar despite differences in muscles, their fiber type, and age. Thus, in the face of considerable overall structural differences of the NMJ, presynaptic to postsynaptic coupling remains constant, as does the relationship between presynaptic vesicles and the nerve terminal branches that support them.** Develop Neurobiol 73: 744–753, 2013

Keywords: **synapse; motor endplate; nerve terminal; acetylcholine; aging**

INTRODUCTION

The neuromuscular junction (NMJ) is often used as a model to study synapse structure and function because of its relative ease of accessibility and its rather simple network of synaptic connectivity (Kummer et al., 2006). Moreover, the NMJ has been shown to be capable of an impressive degree of remodeling, thus providing insight into the nature and characteristics of synaptic plasticity. Indeed, it has been documented that both presynaptic, and postsynaptic morphological alterations of the NMJ are evident following increased, or decreased activity (Pachter and Spielholz, 1990; Deschenes et al., 1993, 2011; Wilson and Deschenes, 2005), as well as being observed as a result of aging (Robbins, 1992; Valdez et al., 2010; Deschenes et al., 2012). Indeed, several experimental techniques have been used to examine age-related remodeling of the NMJ including electron microscopy (Fahim and Robbins, 1982; Banker et al.,

Correspondence to: M.R. Deschenes (mrdesc@wm.edu).

Contract grant sponsor: National Institutes of Health; contract grant number: 9R15AR060637-03.

Contract grant sponsor: Foundation for Aging Studies and Exercise Science Research.

Published online 22 May 2013 in Wiley Online Library (wileyonlinelibrary.com).
DOI 10.1002/dneu.22095

1983), immunofluorescent staining (Deschenes et al., 1993, 2010), as well as electrophysiology (Banker et al., 1983). All of these experimental procedures indicate significant presynaptic and postsynaptic remodeling of the NMJ during the natural process of aging. But in order to ensure functional cell-to-cell communication, proper architectural coupling of the presynaptic nerve terminal (particularly its acetylcholine vesicles) with the postsynaptic endplate region (and its composite acetylcholine receptors) must be maintained. The purpose of the investigation reported here was to determine the efficacy of the NMJ in sustaining presynaptic to postsynaptic structural coupling in skeletal muscles that naturally demonstrate different levels of neuromuscular activity, while examining the NMJs of different muscle fiber types that display disparities in recruitment profiles, and to do so in both young adult, and aged muscles. This approach enabled us to investigate whether NMJs displaying different overall morphological features as determined by their locations in muscles featuring disparate functions, as well as those muscles' constituent fibers which are characterized by different duty cycles (i.e., high vs. low use), are able to maintain proper relationships of presynaptic and postsynaptic features, as well as to assess how aging may alter that ability. As a secondary point of interest, we assessed the relationship between the length of presynaptic nerve terminal branching and the quantity of vesicles supported by a given length of branching, and whether this differed between young and aged muscles, and/or between highly and modestly recruited muscles and their fast- and slow-twitch muscle fibers. We hypothesized that given the considerable differences displayed by NMJs of different muscles and their fiber types, as well as in young vs. aged animals, that presynaptic to postsynaptic structural coupling would similarly vary.

MATERIALS AND METHODS

Subjects

Male Fischer 344 rats, purchased from the National Institutes on Aging Colonies, served as subjects. Hindlimb muscles of 10 young adult (8 months old), and 10 aged (24 months old) rats were used to examine the effects of age and activity patterns on NMJ structure. It is important to note that based upon their average life span, male Fischer 344 rats at 8 and 24 months of age are the age equivalent, respectively, of 23 and 71 year old human males (Turturro et al., 1999; Arias, 2011). Body mass was not found to significantly differ between young adult and aged animals (mean = 396 vs. 402 g, respectively).

Tissue Preparation and Storage

Animals were euthanized and soleus and extensor digitorum longus (EDL) muscles were quickly dissected out, cleared of fat and connective tissue and quickly frozen at resting length in isopentane chilled with liquid nitrogen. Muscles were then stored at -85°C until analysis. The soleus and EDL muscles were selected for study because they demonstrate vastly different duty cycles as the soleus is heavily recruited even during normal daily activity, while the EDL is only sparsely recruited during normal daily activities of living (Hennig and Lomo, 1985). These two muscles also feature stark differences in muscle fiber composition. In the soleus, the predominant fiber type has been shown to be type I (slow-twitch) accounting for 84% of all fibers in that muscle, while in the EDL, the majority of fibers (96%) can be categorized as type II, or fast-twitch (Delp and Duan, 1996).

Cytofluorescent Staining of NMJs

To visualize NMJs, 50-μm-thick longitudinal sections of the middle one-third of the muscle were obtained at -20°C on a cryostat (Cryocut 1800; Reichert-Jung, NuBloch, Germany). To prevent contraction of sections, microscope slides were pretreated in a 3% EDTA solution as previously described (Pearson and Sabarra, 1974). Sections were washed 4×15 min in phosphate buffered saline (PBS) containing 1% bovine serum albumin (BSA). Sections were then incubated in a humidified chamber for 90 min at room temperature in either antifast (for the soleus), or antislow (for the EDL) myosin heavy chain ascites fluid (Sigma Chemical, St. Louis, MO) diluted 1:400. Sections were then washed 4×15 min in PBS with 1% BSA. Tissue was then incubated in AlexaFluor 350 labeled secondary antibody (donkey-raised, anti-mouse IgM, Molecular Probes, Eugene, OR) diluted 1:150 for 90 min in a humidified chamber at room temperature. Sections were then again washed 4×15 min in PBS with 1% BSA before they were incubated overnight at 4°C in supernatant of the primary antibody RT97 (Developmental Studies Hybridoma Bank, University of Iowa), diluted 1:20 in PBS with 1% BSA. The RT97 antibody reacts with nonmyelinated segments of presynaptic nerve terminals (Anderton et al., 1982). The next day, sections were washed 4×15 min in PBS with 1% BSA before being incubated for 2 h at room temperature in fluorescein isothiocyanate-conjugated secondary immunoglobulin (goat-raised, anti-rabbit IgG, Sigma Chemical, St. Louis, MO) which had been diluted 1:150 in PBS with 1% BSA. Sections were then washed 4×15 min in PBS with 1% BSA before being incubated in a humidified chamber overnight at 4°C in a solution containing rhodamine conjugated α-bungarotoxin (BTX; Molecular Probes, Eugene, OR) diluted 1:600 in PBS, along with antisynaptophysin (MP Biomedicals, Solon, OH) at a dilution of 1:50. BTX recognizes postsynaptic acetylcholine (ACh) receptors, while antisynaptophysin reacts with presynaptic vesicles containing ACh. Indeed, synaptophysin is the most abundant protein found in the synaptic vesicular membrane (Kwon and

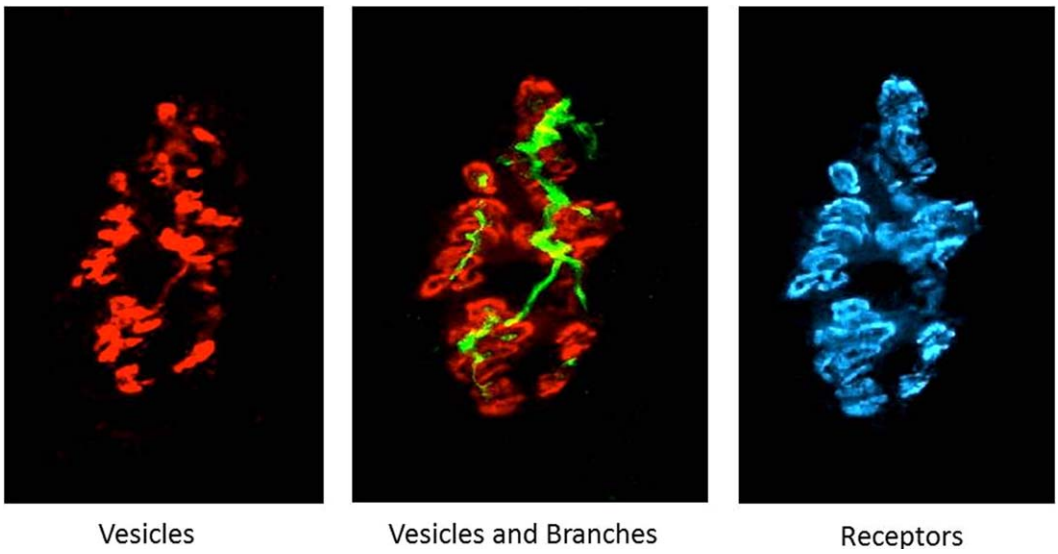

Figure 1 Representative image of fluorescently stained neuromuscular junction. In the far left panel are fluorescently stained presynaptic acetylcholine containing vesicles, in the middle panel are those same vesicles along with associated stained presynaptic nerve terminals, and in the far right panel are fluorescently stained postsynaptic acetylcholine receptors. Original magnification of 1000×. [Color figure can be viewed in the online issue, which is available at wileyonlinelibrary.com.]

Chapman, 2011). The next day, sections were washed 4×15 min in PBS with 1% BSA before incubating them for 2 h in a humidified chamber at room temperature in Alexa-Fluor 647 (goat-raised, anti-rabbit IgG, Molecular Probes, Eugene, OR) labeled secondary antibody to illuminate the antisynaptophysin. Sections were then washed again for 4×15 min before being lightly coated with Pro Long (Molecular probes, Eugene, OR) and having cover slips applied. Slides were then coded with respect to treatment group to allow for blinded evaluation of NMJ morphology and then stored at -20°C until analysis. An example of this cytofluorescent staining of presynaptic and postsynaptic components of the NMJ is displayed in Figure 1.

Presynaptic variables of NMJs assessed included: (1) number of branches identified at the nerve terminal, (2) the total length of those branches, (3) average length per branch, and (4) branching complexity which, as described by Tomas et al. (1990) is derived by multiplying the number of branches by the total length of those branches and dividing that figure by 100. Presynaptic vesicular staining was assessed as: (1) total perimeter, or the length encompassing the entire vesicular region comprised of stained vesicular clusters and nonstained regions interspersed within those clusters, (2) stained perimeter, or the composite length of tracings around individual clusters of vesicles, (3) total area, which includes stained vesicles along with nonstained regions interspersed among vesicle clusters, (4) stained area, or the cumulative areas occupied by ACh vesicular clusters, and (5) dispersion of vesicles, which was assessed by dividing the vesicular stained area by its total area and multiplying by 100. Postsynaptic variables of interest included: (1) total perimeter, or the length encompassing the entire endplate comprised of stained receptor clusters and nonstained regions interspersed within those clusters, (2) stained perimeter, or the composite length of tracings around individual receptor clusters, (3) total area, which includes stained receptors along with nonstained regions interspersed among receptor clusters, (4) stained area, or the cumulative areas occupied by ACh receptor clusters, and (5) dispersion of endplates, which was assessed by dividing the endplate's stained area by its total area and multiplying by 100. See Figure 2 to observe presynaptic and postsynaptic tracings around ACh vesicles and receptors that were generated both manually and by software to assess total and stained perimeter lengths, respectively, and areas contained within those perimeter lengths. The same figure also shows manually traced lengths of branches of nerve terminal endings. In this study, presynaptic to postsynaptic coupling was quantified by dividing the NMJ's postsynaptic stained area by its total length of nerve terminal branching, as well as by quantifying the percentage of the area of postsynaptic staining of receptors that was overlapped with staining of presynaptic ACh vesicles. Finally, to approximate the number of ACh receptors supported by a given length of presynaptic nerve terminal branch length, the stained area occupied by vesicles was divided by the total length of branching for that NMJ.

Histochemical Staining of Myofibers

To quantify muscle fiber profiles, 10-μm-thick transverse sections were obtained from the midbelly of the muscle using a cryostat set at -20°C. This was necessary due to the fact that the longitudinal sections taken to visualize and quantify features of the NMJ are not suitable to assess myofiber size (cross-sectional area) or fiber type composition of

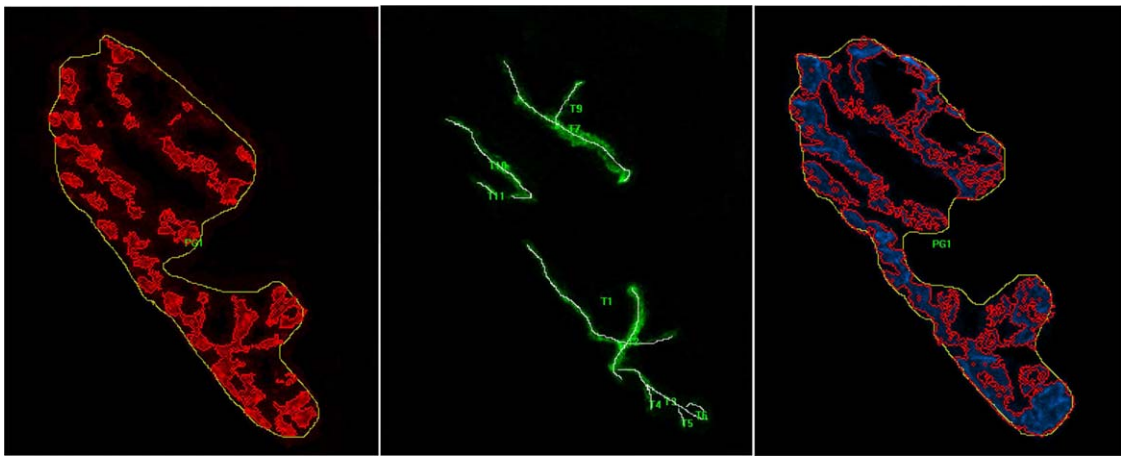

Figure 2 Representative image of tracings used to quantify morphological aspects of the neuromuscular junction. The far left panel depicts tracings (both manually drawn and generated by software) used to quantify presynaptic ACh vesicles, while the middle panel shows tracings used to quantify presynaptic nerve terminal branches. The panel on the far right illustrates tracings made to determine postsynaptic measurements of ACh receptors. Original magnification of 1000×. [Color figure can be viewed in the online issue, which is available at wileyonlinelibrary.com.]

the whole muscle. These cross sections were then stained for myofibrillar ATPase activity following preincubation at a pH of either 4.55 (soleus) or 4.40 (EDL) according to Nemeth and Pette (1981). Although this staining technique allows identification of three fiber types (I, IIA IIX/B), to be consistent with identification of NMJs as either slow- or fast-twitch, fibers were similarly categorized as either type I (slow-twitch), or II (fast-twitch). Slides were coded so that measurements could be conducted in a blinded fashion regarding age group.

Microscopy

An Olympus Fluoview FV 300 confocal system featuring three lasers and an Olympus BX60 fluorescent microscope (Olympus America, Melville, NY) was used to collect images of NMJs and to determine whether they were located on slow- or fast-twitch myofibers. Using a 100× oil immersion objective, it was initially established that the entire NMJ was within the longitudinal borders of the myofiber and that damage to the structure had not occurred during sectioning. A detailed image of the entire NMJ was constructed from a *z*-series of scans taken at 1-μm-thick increments. To determine whether the NMJ resided on a fast- or a slow-twitch myofiber, the fiber was directly viewed from the microscope using the appropriate wavelength to detect the AlexaFluor 350 fluorochrome. Digitized, two-dimensional images of NMJs were stored on the system's hard drive and later quantified with the Image-Pro Plus software (Media Cybernetics, Silver Spring, MD). In the soleus, 10–12 NMJs located on slow-twitch fibers—which dominate in that muscle—were quantified and measurements were averaged to represent slow-twitch NMJs within that muscle. But fast-twitch myofibers are far more sparse in the soleus, so measurements from a minimum of five NMJs were averaged together to represent fast-twitch NMJs of that muscle. Conversely, in the EDL where fast-twitch fibers comprise the majority of muscle mass, 10–12 NMJs residing on those fibers were averaged to represent fast-twitch synapses, while a minimum of five NMJs from the minority slow-twitch myofibers were measured to arrive at mean values for slow type NMJs.

In the quantification of muscle fiber profiles, an Olympus BX41 phase contrast microscope was used in conjunction with a 40× objective. Myofiber cross-sectional areas were quantified with the Image Pro-Express software. A random sample of 125–150 myofibers from each muscle was analyzed to determine average myofiber size (i.e., cross-sectional area) and fiber-type composition (% of total number of fibers examined) for that muscle.

Statistical Analysis

Data are reported as means ± SE. In comparing body mass between young adult and aged rats, an independent *t*-test was conducted. A two-way ANOVA (main effects of muscle fiber type and age) was performed on each NMJ variable of interest. In the event of a significant F ratio for either a main effect or an interactive one, a Fisher protected least squared difference (PLSD) post hoc analysis procedure was conducted to identify significant pairwise differences. In all cases, significance was set at $p < 0.05$.

RESULTS

Soleus NMJs

In examining ANOVA results of NMJ morphology in the soleus, a number of presynaptic and postsynaptic

Table 1 Effects of Age and Muscle Fiber Type on Neuromuscular Junctions of the Soleus

	Young adult		Aged	
	Slow-Twitch	Fast-Twitch	Slow-Twitch	Fast-Twitch
Presynaptic features				
Branch number [a]	15.6 ± 1.2[c]	11.7 ± 1.3	16.2 ± 1.6	13.2 ± 1.8
Total branch length (μm)[a,b]	151.4 ± 9.5[c]	107.2 ± 6.0	180.6 ± 13.6[cd]	129.9 ± 14.0
Average branch length (μm)	11.0 ± 0.8	10.4 ± 0.9	12.1 ± 1.1	12.1 ± 1.7
Branching complexity [a]	28.1 ± 3.3	13.6 ± 1.8	34.0 ± 4.9[c]	20.4 ± 5.4
Vesicle total perimeter (μm)[a]	230.0 ± 17.9	180.5 ± 18.9	250.8 ± 25.5	200.0 ± 24.5
Vesicle stained perimeter (μm)	204.8 ± 14.7	183.5 ± 13.3	220.9 ± 21.0	183.9 ± 18.3
Vesicle total area (μm^2)[a]	499.6 ± 51.3	373.9 ± 35.3	574.4 ± 74.4[c]	385.3 ± 40.3
Vesicle stained area (μm^2)	89.0 ± 9.0	79.4 ± 8.0	102.0 ± 14.7	78.6 ± 9.5
Vesicle dispersion (%)	19.8 ± 1.8	22.4 ± 2.1	19.9 ± 2.5	21.6 ± 1.4
Vesicle area/branch length	0.65 ± 0.08	0.83 ± 0.08	0.65 ± 0.12	0.78 ± 0.10
Postsynaptic features				
Total endplate perimeter (μm)[a]	190.5 ± 9.0[c]	151.1 ± 9.1	221.1 ± 21.4[c]	162.2 ± 11.1
Stained endplate perimeter (μm)[a,b]	270.4 ± 14.1	219.0 ± 13.8	339.6 ± 26.6[cd]	223.8 ± 16.6[d]
Total endplate area (μm^2)[a]	678.2 ± 52.8	570.9 ± 51.1	788.2 ± 80.0[c]	505.8 ± 41.5
Stained endplate area (μm^2)[a]	244.6 ± 18.9	216.1 ± 22.8	265.6 ± 30.4[c]	179.8 ± 23.3
Receptor dispersion (%)	36.2 ± 1.7	33.4 ± 1.2	38.6 ± 3.1	35.3 ± 3.0
Endplate area/branch length	1.74 ± 0.15	2.18 ± 0.18	1.53 ± 0.08	1.87 ± 0.49
Presynaptic to postsynaptic coupling (%)	41.3 ± 3.5	42.2 ± 2.5	43.7 ± 6.8	49.8 ± 4.6

Values are means ± SE.
Branching complexity = branch number × total length/100.
Vesicle dispersion = stained area/total area × 100.
Receptor dispersion = stained area/total area × 100.
Presynaptic to postsynaptic coupling = vesicle stained area/endplate stained area × 100.
[a]Indicates significant ($p < 0.05$) main effect for fiber type.
[b]Indicates significant ($p < 0.05$) main effect for age.
[c]Indicates significant ($p < 0.05$) difference from fast-twitch of same age category.
[d]Indicates significant ($p < 0.05$) difference from young of same fiber type.

features exhibited significant main effects for muscle fiber type, but only two parameters of interest showed a significant main effect for age. Regarding fiber type differences, they were evident in both presynaptic (branch number, total branch length, branching complexity, vesicle total perimeter, vesicle total area), and the postsynaptic (total and stained endplate perimeters, total and stained endplate areas) components of the NMJ. In each of those, it was noted that the size of that variable was significantly greater in slow-twitch compared to fast-twitch muscle fibers. In contrast to the effect of muscle fiber type, only a single presynaptic (total branch length) and postsynaptic (stained endplate perimeter) variable exhibited a main effect for aging whereby values observed among aged NMJs exceeded those of young adult ones.

It was interesting to note that although numerous significant differences occurred in presynaptic and postsynaptic features according to myofiber type and aging, those alterations were tightly linked across the synapse. As a result, measures of presynaptic and postsynaptic coupling were preserved despite those fiber type and aging related differences. More specifically, the dispersion of presynaptic vesicles and postsynaptic receptors were well matched even in the face of differences in myofiber type and age. Moreover, the size of the postsynaptic endplate area relative to the length of presynaptic terminal branching also remained impervious to the effects of muscle fiber type or aging. And finally, the ratio of presynaptic vesicular stained area to the stained area of postsynaptic receptors remained unaffected by differences of myofiber type, or of age. When examining the relationship between presynaptic vesicular stained area and presynaptic nerve terminal branch length, it was revealed that it too, was unaffected by age or muscle fiber type. This indicates that only a certain number of ACh containing vesicles can be anchored for any given length of terminal branching. Results of our analysis of NMJ morphology of the soleus are presented in Table 1.

EDL NMJs

Much like the soleus, a multitude of morphological variables demonstrated significant main effects of

Table 2 Effects of Age and Myofiber Type on Neuromuscular Junctions of the EDL

	Young		Aged	
	Slow-Twitch	Fast-Twitch	Slow-Twitch	Fast-Twitch
Presynaptic features				
Branch number[a,b]	6.6 ± 1.2[c]	12.1± 1.3	10.7 ± 0.7	10.9 ± 1.2
Total branch length (μm)[a]	92.7 ± 9.4[d]	135.1 ± 8.3	101.6 ± 13.1	124.9 ± 8.5
Average branch length (μm)[b]	15.8 ± 1.7	12.5 ± 1.2	10.3 ± 1.6[e]	14.8 ± 1.6
Branching complexity[a]	6.9 ± 1.8[d]	18.2 ± 2.6	12.1 ± 1.7	15.8 ± 2.2
Vesicle total perimeter (μm)[a]	127.2 ± 23.2[d]	210.0 ± 23.9	190.1 ± 19.2	212.8 ± 23.8
Vesicle stained perimeter (μm)[a]	170.0 ± 16.4	224.5 ± 8.9	173.6 ± 16.9[d]	241.0 ± 15.5
Vesicle total area (μm^2)	403.2 ± 93.1	479.8 ± 47.4	356.2 ± 41.7	521.9 ± 78.9
Vesicle stained area (μm^2)[a]	92.1 ± 7.6	94.0 ± 4.0	73.0 ± 8.9[d]	102.3 ± 8.4
Vesicle dispersion (%)	27.5 ± 4.8	22.3 ± 1.5	21.9 ± 2.9	23.8 ± 2.4
Vesicle area/branch length	1.12 ± 0.21	0.81 ± 0.07	0.91 ± 0.19	0.93 ± 0.08
Postsynaptic features				
Total endplate perimeter (μm)	127.8 ± 22.8	159.0 ± 9.9	155.2 ± 12.0	170.5 ± 11.2
Stained endplate perimeter (μm)[a]	177.2 ± 30.7[d]	260.0 ± 20.1	206.4 ± 22.2[d]	290.1 ± 22.4
Total endplate area (μm^2)[a]	488.1 ± 110.8[d]	693.8 ± 36.5	476.5 ± 62.7[d]	711.1 ± 57.7
Stained endplate area (μm^2)[a]	155.7 ± 19.3[d]	269.4 ± 13.6	156.4 ± 31.3[d]	263.0 ± 18.7
Receptor dispersion (%)[a]	34.4 ± 3.3	39.0 ± 1.1	31.0 ± 2.6	37.4 ± 1.7
Endplate area/branch length	2.02 ± 0.48	2.40 ± 0.32	2.01 ± 0.48	2.47 ± 0.18
Presynaptic to postsynaptic coupling (%)[a]	72.1 ± 9.4	41.3 ± 3.6	69.0 ± 20.3	47.4 ± 6.5

Values are means ± SE.
Branching complexity = branch number × total length/100.
Vesicle dispersion = stained area/total area × 100.
Receptor dispersion = stained area/total area × 100.
Presynaptic to postsynaptic coupling = vesicle stained area/endplate stained area × 100.
[a]Indicates significant ($p < 0.05$) main effect for fiber type.
[b]Indicates significant ($p < 0.05$) effect for interaction between fiber type and age.
[c]Indicates significant ($p < 0.05$) difference from all three other groups.
[d]Indicates significant ($p < 0.05$) difference from fast-twitch of same age category.
[e]Indicates significant ($p < 0.05$) difference from young, slow-twitch and aged, fast-twitch.

muscle fiber type; in fact a greater number than that observed in the soleus. But unlike the soleus, not a single synaptic parameter quantified demonstrated a main effect for age. It is also noteworthy that in the EDL the NMJs of fast-twitch fibers were significantly larger than those of the slow-twitch fibers. This is the polar opposite to what was found in the soleus where NMJ dimensions of slow-twitch myofibers exceeded those of fast-twitch fibers. Yet similar to what was detected in the soleus, it was confirmed that while NMJ parameters of the EDL showed considerable variability according to fiber type, presynaptic to postsynaptic coupling was well maintained. Thus, even though the NMJs of the soleus and EDL display sharp structural differences and specificity to muscle fiber type, presynaptic to postsynaptic coupling is conserved with equal fidelity in both of those muscles. Although a main effect of fiber type was noted on the dispersion of postsynaptic receptors, as well as the degree of overlap between presynaptic vesicles with those same postsynaptic receptors, post hoc analyses failed to detect any significant pairwise differences for either of those variables. Results of our NMJ analysis in the EDL can be found in Table 2.

Myofiber Profiles

In quantifying myofiber size (cross-sectional area) of the soleus, it was found that with fiber types collapsed together, the average size of aged fibers was ~13% less than that of young adult soleus fibers ($p < 0.005$). Similarly, when solely examining the type I, or slow-twitch fibers that are predominantly expressed in the soleus, it was revealed that those fibers were significantly smaller—by about 12%—than those fibers in young adult soleus muscles. And when assessing the type II (fast-twitch) myofibers of the soleus, it was once again noted that aging was associated with significant atrophy, but to an even more pronounced degree, i.e., ~42%. It was also determined, not surprisingly, that aging was associated with alterations in the myofiber composition of

Table 3 Myofiber Profiles of Young Adult, and Aged Soleus and EDL Muscles

	Soleus			EDL	
	Cross-Sectional Area (μm^2)	% Composition		Cross-Sectional Area (μm^2)	% Composition
Types combined			Types combined		
Young	2518.4 ± 74.6[a]		Young	2266.2 ± 113.9[a]	
Aged	2182.4 ± 71.1		Aged	1875.0 ± 85.1	
Type I			Type I		
Young	2512.5 ± 79.9[a]	88.7 ± 1.2[b]	Young	1199.3 ± 104.2	10.8 ± 1.2[b]
Aged	2202.8 ± 83.5	92.6 ± 1.6	Aged	1042.3 ± 39.1	15.4 ± 2.0
Type II			Type II		
Young	2777.5 ± 122.3[a]	11.3 ± 0.8[a]	Young	2540.6 ± 115.6[a]	89.2 ± 1.5[a]
Aged	1605.3 ± 131.9	7.4 ± 0.9	Aged	2216.3 ± 92.4	84.6 ± 2.3

Values are means ± SE.
[a]Indicates significant difference ($p < 0.05$) from aged for that variable in that muscle (i.e., soleus or EDL).
[b]Indicates a trend ($p = 0.06$) for a difference from aged for that variable in that muscle (i.e., soleus or EDL).

the soleus. Specifically, there was a significant decrease in the percentage of fast-twitch fibers in aged solei compared to young ones (7.4 vs. 11.3%, respectively).

As with the primarily slow-twitch soleus, the mainly fast-twitch EDL muscle also demonstrated significant age-related effects on myofiber size, and fiber-type distribution. With fiber types pooled together, a 17% decline in average fiber cross-sectional area was detected among aged EDL muscles relative to young adult EDLs. And when assessing individual fiber types, the type II myofibers of aged EDL muscles displayed a significant reduction in size on the order of roughly 13%. In contrast, the minority type I fibers of the EDL did not exhibit a significant aging-related decrement in size. With respect to muscle fiber composition, as with the soleus, aged EDL muscles featured a greater proportion of type I fibers (aged = 15.4%, young = 10.8%) with a concomitant, and significant, loss in the percentage of type II, or fast-twitch, myofibers expressed (aged = 84.6%, young = 89.2%). Detailed myofiber profiles of soleus and EDL muscles are presented in Table 3.

DISCUSSION

One of the cardinal features of the NMJ is its ability to remodel itself as a result of changes in activity, development, and aging (Collins and DiAntonio, 2007; Deschenes, 2011; Valdez et al., 2012). Structurally, alterations may include modified length of nerve terminal branching, number and distribution of presynaptic vesicles containing ACh, as well as in the number and distribution of postsynaptic receptors for ACh (Covault and Sanes, 1986; Deschenes et al., 1993, 2011; Missias et al., 1996; Vock et al., 2008). Yet at the same time, for effective synaptic communication to occur, the physical relationship between vesicles containing neurotransmitter and their postsynaptic binding sites (receptors) must be effectively maintained. This is essential because once released into the synaptic cleft, ACh can only passively diffuse across that physical separation of the presynaptic and postsynaptic components of the NMJ. Accordingly, it is simply a matter of probability as to whether ACh successfully diffuses across the synapse and binds to an unoccupied postsynaptic receptor so that it can trigger first depolarization, and then contraction of the involved muscle fiber. Of course, this probability increases as the distance between the release and binding sites is minimized, and the relationship between presynaptic ACh containing vesicles and postsynaptic ACh binding sites (receptors) remains stable.

The primary question driving this investigation was whether the relationship between presynaptic and postsynaptic structure was effectively maintained in muscles—and their muscle fibers—demonstrating dramatic differences in patterns of habitual use, and to do so in both young adult and aged animals. Like differences in physical activity, aging has also been shown to elicit NMJ remodeling (Anis and Robbins, 1987; Robbins, 1992; Nishimune, 2012) potentially disturbing proper presynaptic to postsynaptic structural relationships.

Our results were both surprising and expected. That is, our ANOVA procedures consistently detected significant differences in NMJ dimensions in slow- and fast-twitch myofibers in both the heavily recruited soleus, as well as in the lightly recruited EDL muscle, but only rarely identified were age-related differences in NMJ morphology. Perhaps the

rats used here—while considered aged—were simply not old enough to have experienced extensive age-related NMJ reconfiguration. It is important to note, however, that the expected age-related alterations in myofiber profiles of the soleus and the EDL were observed in the present investigation. That is, in both the soleus and the EDL, the sarcopenic effects of aging were manifested as myofiber atrophy and a decline in the expression of fast-twitch fibers, as they have been previously reviewed (Deschenes, 2004; Kostek and Delmonico, 2011). Still, these modifications in myofiber size and type were not linked with changes in morphological parameters of NMJs. This uncoupling of modifications of NMJs and their muscle fibers has been reported before, but typically in response to pronounced changes in the amounts of physical activity performed (Deschenes et al., 1993, 2011).

When examining more closely the effect of muscle fiber type on NMJ architecture, it was interesting to note that although a main effect was noted in both the soleus and the EDL muscles, the fiber type that expressed larger NMJs was reversed among those two muscles. More specifically, in the soleus, NMJ dimensions were larger among the predominantly expressed slow-twitch fibers compared to fast-twitch ones, while in the EDL where fast-twitch fibers are in the majority, it was the NMJs of those fast-twitch muscle fibers that were found to be greater in magnitude. These results of NMJ structure from the EDL would appear to be in contrast with earlier evidence suggesting that greater amounts of physical activity—and thus neurotransmission—result in the expansion of presynaptic and postsynaptic structure. Presumably, this adaptation allows the NMJ to store more ACh as well as express a greater number of receptors for that neurotransmitter which, in turn, would help delay the onset of neuromuscular transmission failure and its resultant muscular fatigue. Our observations gathered from the primarily slow-twitch soleus are consistent with that paradigm. This, however, would not be supported by our data collected from the EDL. Even though slow-twitch myofibers are in the minority in that principally fast-twitch muscle, it is still the slow-twitch fibers that are first to be recruited during the activation of the EDL. This is dictated by the size principal of motor unit recruitment during voluntary muscle contractile activity (Henneman, 1957; Henneman et al., 1974). Nevertheless, our results from the EDL clearly show that it is the predominantly expressed fast-twitch myofibers that exhibit larger NMJ architectural features compared to the minority slow-twitch fibers. Perhaps it is because there is such a dearth of slow-twitch fibers comprising the EDL that during even normal contractile activity for that muscle fast-twitch fibers must be recruited and thus undergo NMJ expansion. More likely though, it is the previously established relationship between the size of myofibers and the NMJs residing on them first reported by Balice-Gordon and Lichtman (1990; 1993) observed in young, developing mice that accounts for the specificity of NMJ size in the soleus and EDL. That is, in the soleus, it is the slow-twitch fibers that are most impressive in size (when age groups are collapsed together), while in the EDL not only is the greatest percentage of fibers accounted for by the fast-twitch variety, but the average size of fast-twitch fibers exceeds that of slow-twitch fibers (Delp and Duan, 1996). This would suggest that larger muscle fibers are structurally obliged to have larger NMJs as well (Balice-Gordon et al., 1990).

Despite the consistent and considerable differences in NMJ morphology between slow- and fast-twitch muscle fibers in both the soleus and the EDL, the results presented here underscore a remarkable precision of presynaptic to postsynaptic morphological coupling when measured as the ratio of motor endplate area relative to nerve terminal length. Indeed, this measure of coupling remained constant across muscle (soleus and EDL), muscle fiber type (slow- and fast-twitch), as well as age (young adult and aged). And although a significant main effect for fiber type was noted in the EDL—no such main effect was evident in the soleus—when presynaptic to postsynaptic coupling was assessed as the degree of overlap between stained presynaptic ACh containing vesicles with postsynaptic stained receptors, post hoc analysis failed to identify any significant, direct pair-wise differences. This was true even though the statistically powerful Fisher PLSD was used as the post hoc procedure. It is reasonable then, to conclude that presynaptic to postsynaptic structural coupling was stable across age, and fiber type among the soleus and EDL muscles.

The morphological data presented here demonstrating maintenance of presynaptic to postsynaptic structural relationships are consistent with findings from earlier works on the effect of aging on neuromuscular transmission using electrophysiological techniques. In at least two different investigations it was determined that aging did not significantly alter the amplitude of either mini endplate potentials (i.e., spontaneous release of neurotransmitter at the NMJ), or the amplitude of electrically stimulated endplate potentials (Banker et al., 1983; Kelly and Robbins, 1986). It is quite possible that the stability of presynaptic to postsynaptic coupling of the NMJ noted here

in young and aged rats contributes to the maintenance of the strength of neuromuscular transmission observed in those earlier studies.

The staining procedure developed for this study enabled us to examine three different aspects of NMJ structure (i.e., presynaptic branching, presynaptic vesicles, postsynaptic receptors) and to do so in a muscle fiber type specific manner (slow- vs. fast-twitch). This newly employed staining procedure was particularly beneficial in that it allowed us to examine the relationship between presynaptic vesicles and the nerve terminal branches to which those vesicles are attached. It has been demonstrated that changes in activity result both in alterations in branching patterns (Deschenes et al., 2006, 2011) and the presynaptic area occupied by vesicles (Andonian and Fahim, 1988; Fahim, 1997). By employing fluorochromes of four different wavelengths, and three lasers to capture images of the three NMJ features alluded to above, we were able to gain insight into the relationship not only of the effects of activity and aging on presynaptic to postsynaptic adaptations, but also into the more detailed relationships between presynaptic nerve terminal branching and presynaptic ACh containing vesicles supported by those branches. Specifically assessed here was the morphological relationship between vesicles and branches (See Fig. 1, middle panel) in muscles differing with respect to duty cycles (soleus vs. EDL), as well as the heavily and lightly recruited myofibers (slow- vs. fast-twitch) that comprise those muscles, along with being able to examine the effect of aging on those relationships. In a crude real life corollary, the question we wanted to answer was whether it was necessary for an apple tree to form a greater total length of its branching network if it was to hold more fruit, or could more apples simply be packed onto the preexisting total branch length. The data presented here confirm that regardless of the muscle, the myofiber type in that muscle, or even the age of the muscle, the ratio of the number of vesicles attached to any given unit of branch length is firmly maintained. In this study, the number of vesicles was indirectly estimated by assessing the area of vesicular staining while assuming, as previously indicated (Heuser et al., 1979; Richards et al., 2003; Rizzoli and Betz, 2004) that the size of individual vesicles is not subject to change. Thus, to store more neurotransmitter in the presynaptic nerve terminal region it is imperative that total branch length must be increased commensurately. The factors and molecular signals that allow this tightly maintained ratio of vesicles to branch length remain to be elucidated.

In summary, the results presented here not only confirm what has been previously reported regarding the fiber type specificity of NMJ structure, they also elaborate on those findings. Here, we observed the capacity of the NMJ to maintain tight coupling of its presynaptic and postsynaptic morphological features despite substantial overall structural differences among synapses located in different myofiber types. Further, it was revealed that even when displaying significant differences in nerve terminal branching and area occupied by neurotransmitter containing vesicles, the ratio of those vesicles secured by a given length of branching is robustly regulated. It is evident then that even though dramatic overall remodeling of the NMJ may occur, the maintenance of relationships between presynaptic and postsynaptic morphological features, along with the number of presynaptic vesicles supported by a given length of nerve terminal branching, is of the highest priority. This impressive ability to preserve presynaptic to postsynaptic features of the NMJ during the early stage of aging may have important implications regarding a number of serious health issues confronting our growing population of seniors. That is, recent studies have demonstrated a link between the structural deterioration of the NMJ and diabetes, sarcopenia, osteoporosis, and even cancer (Lesniewski et al., 2003; Shigemoto et al., 2010). Thus, by maintaining proper presynaptic to postsynaptic patterning of the NMJ during the early stages of senescence, it may be possible to delay, or even avoid, the onset of these serious age-related health and quality of life impairments. Further investigation will be needed to determine this.

REFERENCES

Anderton BH, Breinburg D, Downes MJ, Green PJ, Tomlinson BE, Ulrich J, Wood JN, Kahn J. 1982. Monoclonal antibodies show that neurofibrillary tangles and neurofilaments share antigenic determinants. Nature 298:84–86.

Andonian MH, Fahim MA. 1988. Endurance exercise alters the morphology of fast- and slow-twitch rat neuromuscular junctions. Int J Sports Med 9:218–223.

Anis NA, Robbins N. 1987. General and strain-specific age changes at mouse limb neuromuscular junctions. Neurobiol Aging 8:309–318.

Arias E. 2011. United States life tables, 2007. Natl Vital Stat Rep 59:1–60.

Balice-Gordon RJ, Breedlove SM, Bernstein S, Lichtman JW. 1990. Neuromuscular junctions shrink and expand as muscle fiber size is manipulated: In vivo observations in the androgen-sensitive bulbocavernosus muscle of mice. J Neurosci 10:2660–2671.

Balice-Gordon RJ, Lichtman JW. 1993. In vivo observations of pre- and postsynaptic changes during the transition from multiple to single innervation at developing neuromuscular junctions. J Neurosci 13:834–855.

Balice-Gordon RJ, Lichtman JW. 1990. In vivo visualization of the growth of pre- and postsynaptic elements of neuromuscular junctions in the mouse. J Neurosci 10:894–908.

Banker BQ, Kelly SS, Robbins N. 1983. Neuromuscular transmission and correlative morphology in young and old mice. J Physiol 339:355–377.

Collins CA, DiAntonio A. 2007. Synaptic development: Insights from drosophila. Curr Opin Neurobiol 17:35–42.

Covault J, Sanes JR. 1986. Distribution of N-CAM in synaptic and extrasynaptic portions of developing and adult skeletal muscle. J Cell Biol 102:716–730.

Delp MD, Duan C. 1996. Composition and size of type I, IIA, IID/X, and IIB fibers and citrate synthase activity of rat muscle. J Appl Physiol 80:261–270.

Deschenes MR. 2004. Effects of aging on muscle fibre type and size. Sports Med 34:809–824.

Deschenes MR. 2011. Motor unit and neuromuscular junction remodeling with aging. Curr Aging Sci 4:209–220.

Deschenes MR, Maresh CM, Crivello JF, Armstrong LE, Kraemer WJ, Covault J. 1993. The effects of exercise training of different intensities on neuromuscular junction morphology. J Neurocytol 22:603–615.

Deschenes MR, Roby MA, Glass EK. 2011. Aging influences adaptations of the neuromuscular junction to endurance training. Neuroscience 190:56–66.

Deschenes MR, Sherman EG, Glass EK. 2012. The effects of pre-habilitative conditioning on unloading-induced adaptations in young and aged neuromuscular systems. Exp Gerontol 47:687–694.

Deschenes MR, Tenny KA, Wilson MH. 2006. Increased and decreased activity elicits specific morphological adaptations of the neuromuscular junction. Neuroscience 137:1277–1283.

Fahim MA. 1997. Endurance exercise modulates neuromuscular junction of C57BL/6NNia aging mice. J Appl Physiol 83:59–66.

Fahim MA, Robbins N. 1982. Ultrastructural studies of young and old mouse neuromuscular junctions. J Neurocytol 11:641–656.

Henneman E. 1957. Relation between size of neurons and their susceptibility to discharge. Science 126:1345–1347.

Henneman E, Clamann HP, Gillies JD, Skinner RD. 1974. Rank order of motoneurons within a pool: Law of combination. J Neurophysiol 37:1338–1349.

Hennig R, Lomo T. 1985. Firing patterns of motor units in normal rats. Nature 314:164–166.

Heuser JE, Reese TS, Dennis MJ, Jan Y, Jan L, Evans L. 1979. Synaptic vesicle exocytosis captured by quick freezing and correlated with quantal transmitter release. J Cell Biol 81:275–300.

Kelly SS, Robbins N. 1986. Sustained transmitter output by increased transmitter turnover in limb muscles of old mice. J Neurosci 6: 2900-2907.

Kostek MC, Delmonico MJ. 2011. Age-related changes in adult muscle morphology. Curr Aging Sci 4:221–233.

Kummer TT, Misgeld T, Sanes JR. 2006. Assembly of the postsynaptic membrane at the neuromuscular junction: Paradigm lost. Curr Opin Neurobiol 16:74–82.

Kwon SE, Chapman ER. 2011. Synaptophysin regulates the kinetics of synaptic vesicle endocytosis in central neurons. Neuron 70:847–854.

Lesniewski LA, Miller TA, Armstrong RB. 2003. Mechanisms of force loss in diabetic mouse skeletal muscle. Muscle Nerve 28:493–500.

Missias AC, Chu GC, Klocke BJ, Sanes JR, Merlie JP. 1996. Maturation of the acetylcholine receptor in skeletal muscle: Regulation of the AChR gamma-to-epsilon switch. Dev Biol 179:223–238.

Nemeth P, Pette D. 1981. Succinate dehydrogenase activity in fibres classified by myosin ATPase in three hind limb muscles of rat. J Physiol 320:73–80.

Nishimune H. 2012. Active zones of mammalian neuromuscular junctions: Formation, density, and aging. Ann N Y Acad Sci 1274:24–32.

Pachter BR, Spielholz NI. 1990. Tenotomy-induced motor endplate alterations in rat soleus muscle. Anat Rec 228: 104–108.

Pearson J, Sabarra A. 1974. A method for obtaining longitudinal cryostat sections of living muscle without contraction artifacts. Stain Technol 49:143–146.

Richards DA, Guatimosim C, Rizzoli SO, Betz WJ. 2003. Synaptic vesicle pools at the frog neuromuscular junction. Neuron 39:529–541.

Rizzoli SO, Betz WJ. 2004. The structural organization of the readily releasable pool of synaptic vesicles. Science 303:2037–2039.

Robbins N. 1992. Compensatory plasticity of aging at the neuromuscular junction. Exp Gerontol 27:75–81.

Shigemoto K, Kubo S, Mori S, Yamada S, Akiyoshi T, Miyazaki T. 2010. Muscle weakness and neuromuscular junctions in aging and disease. Geriatr Gerontol Int 10: S137–S147.

Tomas J, Fenoll R, Mayayo E, Santafe M. 1990. Branching pattern of motor nerve endings in a skeletal muscle of the adult rat. J Anat 168:123–135.

Turturro A, Witt WW, Lewis S, Hass BS, Lipman RD, Hart RW. 1999. Growth curves and survival characteristics of the animals used in the biomarkers of aging program. J Gerontol A Biol Sci Med Sci 54: B492-501.

Valdez G, Tapia JC, Kang H, Clemenson GD Jr, Gage FH, Lichtman JW, Sanes JR. 2010. Attenuation of age-related changes in mouse neuromuscular synapses by caloric restriction and exercise. Proc Natl Acad Sci U S A 107: 14863–14868.

Valdez G, Tapia JC, Lichtman JW, Fox MA, Sanes JR. 2012. Shared resistance to aging and ALS in neuromuscular junctions of specific muscles. PLoS One 7:e34640.

Vock VM, Ponomareva ON, Rimer M. 2008. Evidence for muscle-dependent neuromuscular synaptic site determination in mammals. J Neurosci 28:3123–3130.

Wilson MH, Deschenes MR. 2005. The neuromuscular junction: Anatomical features and adaptations to various forms of increased, or decreased neuromuscular activity. Int J Neurosci 115:803–828.